World Scientific
www.worldscientific.com

Layout Optimization of Ill-Loaded Multiphase Bi-Modulus Materials

Kun Cai

College of Water Resources and Architectural Engineering
Northwest A&F University, Yangling 712100, P. R. China

Research School of Engineering
the Australian National University ACT, 2601, Australia
kuicansj@163.com

Jing Cao[*] and Jiao Shi[†]

College of Water Resources and Architectural Engineering
Northwest A&F University, Yangling 712100, P. R. China
[*]caojingxn@163.com
[†]shijiao8@sohu.com

Qing H. Qin

Research School of Engineering
the Australian National University, ACT, 2601, Australia
qinghua.qin@anu.edu.au

The optimal layouts of multiple bi-modulus materials in a continuum under ill-loaded cases are found using the scheme of fractional-norm (Q-norm and Q is in (0, 1)) weighting objective function. The major ideas of the present study are as follows. First, the bi-modulus material topology optimization is solved using material replacement approach. Second, the power-law scheme is adopted to express the equivalent stiffness of multiple materials. Third, the ill-loaded topology optimization is solved by changing the value of Q. Combining the three techniques, a feasible solution for the ill-loaded structural optimization can be found even when there are many bi-modulus materials. Numerical tests are presented to show the characters of the materials layout in the structure.

Keywords: Multi-material layouts; bi-modulus; multiple loading cases; fractional-norm weighting scheme; ill-loaded cases.

1. Introduction

Topology optimization is a powerful computational tool in variety of design fields such as acoustics structure [Dühring *et al.*, 2008], crashworthiness equipment [Forsberg and Nilsson, 2007], fluidics devices [Gersborg-Hansen *et al.*, 2005], micro-electro- mechanical systems [Jang *et al.*, 2008], and heat transfer system [Zhuang *et al.*, 2007] during last two decades. In a practical design, two types of problem are

very popular. One is that there are many materials in the design domain. The other is that the structure is in operation under different loading conditions. Hence, the theoretical and numerical study on optimization of such problems is important.

For the first problem, it is a typical multiple materials layout optimization. To solve such optimization problem, many strategies have been proposed, including the solid isotropic microstructure with penalization (SIMP) method [Gibiansky and Sigmund, 2000; Qin and He, 1995; Sigmund and Torquato, 1999], the level set method (LSM) [Allaire *et al.*, 2013; Mei and Wang, 2004; Wang and Wang, 2004], the evolutionary structural optimization (ESO) method (Han and Lee, 2005), the discrete material optimization (DMO) method [Blasques and Stolpe, 2012; Hvejsel and Lund, 2011; Stegmann and Lund, 2005], the phase field method [Wang and Zhou, 2005; Zhou and Wang, 2006], and the "pseudo-sensitivities" approach by [Ramani, 2009]. Especially, finding an optimal layout of multiple material with simple material interfaces is important when considering the manufacturing constraints [Guo *et al.*, 2014a, 2014b; Natasha *et al.*, 2014; Zhou and Wang, 2013]. To the authors' knowledge, multiple bi-modulus materials layout optimization under ill-loaded cases is not considered in the work mentioned above.

On the other hand, a bi-modulus material is such a material that its tensile modulus is not equal to the compressive one in a given direction. It widely exists in practical engineering, such as the concrete in civil engineering or cast iron in mechanical engineering. The constitutive curve of a bi-modulus material is piece-wise linear, which implies that the constitutive property of the material is stress-dependent. Due to wide applications of such bi-modulus materials as foam [Zenkert and Burman, 2009], graphites [Seldin, 1966], concrete [Bruggi, 2014; Yang *et al.*, 2014], etc., many work has been reported in investigating deformation behavior of a bi-modulus structure since the mid of last century [Ambartsumyan, 1965; Du and Guo, 2014; Jones, 1977; Kanno, 2011]. Recently, Du and Guo [2014] constructed a variational principle for modeling such boundary problems. They stated that the accurate deformation of a bi-modulus structure can, theoretically, be found efficiently using the state-of-the-art variational principles. Besides, topology optimization model of a bi-modulus structure has also been reported in the past decades. For example, based on ground structure method [Dorn, 1964], Achtziger [1996] discussed the optimal topology of a truss structure with different tension/compression properties. Chang *et al.* [2007] approximated the original piece-wise linear stress-strain curve with a derivable nonlinear curve of a bi-modulus material in layout optimization of a tension/compression only material (e.g., cable or membrane). Similarly, Liu and Qiao [2010] used Heaviside function to describe the dual tension/compression moduli of a bi-modulus material proprieties in a structure with large deformation. For layout optimization with tension/compression-only material, Cai and Shi [2008] presented a heuristic approach to solve the bi-modulus material problem. After that, Cai *et al.* [2013] provide a modified SIMP method to solve the same problem. For a truss-like

continua, Querin *et al.* [2010] suggested an optimality criterion (OC) based method for layout optimization of a bi-modulus material.

It is noted that only stiffness design rather than strength design [Bruggi and Duysinx, 2013; Luo and Kang, 2013; Luo *et al.*, 2015] has been involved in the above works. It should also be mentioned that the piece-wise linear property of a bi-modulus material should also be considered in the deformation analysis of a structure which such a material is involved in the design using topology optimization. In general, the bi-modulus material shows linear and isotropic when it is under either pure tension or pure compression state. The accurate deformation of a continuum structure with isotropic material(s) can, obviously, be found without reanalysis/iteration. However, if the bi-modulus material is under complex state, i.e., neither pure tension nor pure compression, the material shows transversal isotropic and the normal of isotropic plane depends on the direction of the second principal stress. It is the major reason for the complexity of deformation analysis of a bi-modulus structure, i.e., structural reanalysis is required. Fortunately, if the bi-modulus structure is in a design domain of topology optimization, the iteration for updating the design variables can also be used for finding the accurate deformation of the bi-modulus in the design domain, simultaneously. According to this idea, Cai *et al.* [2011, 2013] replaced the original bi-modulus material with two isotropic materials in topology optimization of a bi-modulus structure. This scheme is also adopted in the present study.

It is noted from above review that very few work was involved in multiple load cases (MLC). In fact, for most structures/devices, they are run under several types of loading cases. The optimization of such structures/devices is a typical multi-objective optimization. In general, a generalized objective function is constructed to convert the original multi-objective optimization into a single objective optimization. For instance, in the work by Díaz and Bendsøe [1992], the scheme of a linear weighted objective function of the mean compliances of structure under MLC was suggested. Luo *et al.* [2006] presented a square weighting scheme for topology optimization by considering both static and dynamic loadings. However, when the magnitude of the weakest load is far less than that of the strongest load and the weakest load is not on the load transfer path (LTP) of strongest load, there is no material to support the weakest load in the final design. Such MLC is usually known as ill-load cases (ILC). To overcome the difficulty, Sui *et al.* [2000] classified the loads into two levels according to load magnitudes, and the topology optimization is carried out on the two levels alternatively. Obviously, the final solution depends on the classification scheme of the two levels. Cai *et al.* [2014] presented a fractional-norm weighting scheme for solving the problem of ill-loaded topology optimization. Their results indicated that a feasible solution can be found when the order of norm is in $[0.1, 0.5]$ even if the magnitude of the weakest load is only 0.1% of the strongest load. But their solution is applied in an isotropic structure under ILC only.

In this work, a layout optimization model is presented for analyzing multiple bi-modulus materials under ILC. It is organized as follows: In Sec. 2, details of the proposed methodology are described. In Sec. 3, four typical examples are studied numerically. Finally, some conclusions are presented in Sec. 4.

2. Methodology

2.1. *Basic equations for linear elasticity problem*

Consider a solution domain $\mathbf{\Omega} \subseteq \mathbf{R}^2$ or $\mathbf{R}^3$ with Dirichlet boundary (Γ_1) and Neumann boundary (Γ_2 and $\Gamma_1 \cup \Gamma_2 = \partial\mathbf{\Omega}$), the deformation is governed by the following equations.

- Equilibrium equation

$$- \nabla \cdot \boldsymbol{\sigma}(\mathbf{u}) = \mathbf{f} \quad \text{in } \mathbf{\Omega}. \tag{1}$$

- Strain–displacement relationship

$$\boldsymbol{\varepsilon}(\mathbf{u}) = \frac{1}{2}[\nabla\mathbf{u} + (\nabla\mathbf{u})^T]. \tag{2}$$

- Constitutive relationship

$$\boldsymbol{\sigma}(\mathbf{u}) = \mathbf{D} : \varepsilon(\mathbf{u}). \tag{3}$$

- Displacement boundary condition

$$\mathbf{u} = \mathbf{u}_0. \tag{4}$$

- Force boundary condition

$$\boldsymbol{\sigma}(\mathbf{u}) \cdot \mathbf{n} = \mathbf{T}, \tag{5}$$

where $\boldsymbol{u}$ is the displacement vector, $\boldsymbol{\sigma}$ the stress tensor, $\boldsymbol{f}$ the body force vector, $\boldsymbol{\varepsilon}$ the strain tensor, $\boldsymbol{u}_0$ the specified displacement vector on Γ_1, and $\boldsymbol{T}$ the contact force vector on Γ_2. $\boldsymbol{D}$ is the elasticity tensor of the material. In the present work, finite element method (FEM) is utilized to solve the above partial-differential equations (PDEs).

2.2. *Interpolation scheme of multiple materials*

In topology optimization of a structure with multiple bi-modulus materials, density-based method, e.g., the SIMP approach, is adopted after material replacement operation [Cai *et al.*, 2013] in the present study. Thus, the exact relationship between the equivalent elasticity of the mixture in a finite element and the properties of the component materials in the element should be given.

For a typical topology optimization problem with only one solid material in design domain, the power-law interpolation scheme is defined as

$$E^{(1)}(\rho_{1,j}) = \rho_{1,j}^{p} E_1.\tag{6}$$

where $\rho_{1,j} \in [0,1]$ is the design variable of the jth element, E_1 is the material modulus of the solid, and p (typically $p=3$) is the penalization parameter.

Assume that the total number of materials in design domain is m, whose elastic moduli are $E_1 \geq E_2 \ldots \geq E_m$, respectively. The equivalent modulus $E^{(m)}$ can be calculated using the following recursion formulation

$$E^{(m)}(\rho_{1,j}, \rho_{2,j}, \ldots, \rho_{m-1,j}) = \rho_{m-1,j}^{p}(E^{(m-1)}) + (1 - \rho_{m-1,j}^{p})E_m.\tag{7}$$

where $\rho_{i,j}(i = 1, 2, \ldots, m - 1)$ is the ratio of the first i types of materials over the first $(i + 1)$ types of materials in the jth element in design domain.

2.3. *Mathematical formulation for optimization*

For a multi-phases material optimization under MLC, the optimization problem described above can be formulated as

$$
\begin{aligned}
&\textbf{Find} \quad \{\rho_{i,j} | i = 1, 2, \ldots, m - 1; j = 1, 2, \ldots, N_{\text{EL}}\} \\
&\textbf{min} \quad c_w = \left[\sum_{\text{lc}=1}^{N_{\text{LC}}} (w_{\text{lc}} \overline{c_{\text{lc}}})^{Q} \right]^{1/Q}, \\
&\textbf{s.t.} \quad \sum_{j=1}^{N_{\text{EL}}} \psi_{i,\,j} \cdot v_j = V_0 \cdot f_i, \quad (i = 1, 2, \ldots, m - 1) \\
&\qquad \sum_{\text{lc}=1}^{N_{\text{LC}}} w_{\text{lc}} = 1.0, \\
&\qquad K_{\text{lc}} \cdot U_{\text{lc}} = P_{\text{lc}}, \quad (\text{lc} = 1, 2, \ldots, N_{\text{LC}}) \\
&\qquad 0 < \rho_{\min} \leq \forall \rho_{i,j} \leq 1, \\
&\qquad w_{\text{lc}} \geq 0, Q > 0,
\end{aligned}\tag{8}
$$

where c_w is the generalized objective function which is the weighted structural compliance under MLC. w_{lc} is the linear weighting coefficient of the lcth loading case. Q is the power exponent for weighting scheme. N_{LC} is number of MLC. P_{lc} and U_{lc} denote the global nodal force and global displacement vectors in the lcth load case respectively. K_{lc} is the stiffness matrix which can be formed using the well-established FEM [Bathe, 2006; Qin, 1994; 1995; 2005], N_{EL} is the total number of elements in the design domain. m is number of materials. v_j is the volume of the jth element, f_i is the volume fraction of the ith material, V_0 stands for the total volume of design domain. $\rho_{\min}$ is the minimum relative densities to avoid singularity ($\rho_{\min} = 0.001$ is used in our analysis). For the case of $i = 1$, ρ_0 is zero. $\psi_{i,j}$ is the
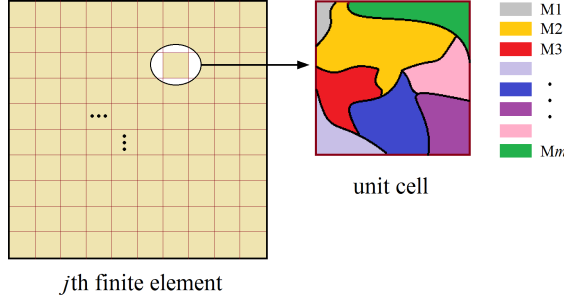
Fig. 1.   Diagram of multi-phases materials in a finite element.

volume ratio of the ith material to the jth element (Fig. 1), and the relationship between $\psi_{i,j}$ and $\rho_{i,j}$ is expressed as

$$\psi_{i+1,j} = \frac{1 - \rho_{i,j}}{\rho_{i,j}(1 - \rho_{i-1,j})}\psi_{i,j}. \qquad (9)$$

2.4. *Moduli selection of local isotropic materials*

In an uniaxial mechanics test, the elasticity of a bi-modulus material under tension is different from that of the same sample under compression. Assuming E_T to be the tensile modulus and E_C the compressive modulus, the ratio between E_T and E_C is defined as

$$R_{\text{TCE}} = \frac{E_T}{E_C}. \qquad (10)$$

To solve topology optimization problem defined in Eq. (8), two levels of iterations are required. In the inner loop, the accurate deformation of the nonlinear structure with many bi-modulus materials is obtained, whereas in the outer one the updated design variables in optimization is implemented. To merge the inner loop into the outer loop, we adopt the material replacement operation, i.e., to replace the original bi-modulus materials with corresponding isotropic materials during deformation analysis before topology optimization is performed. Noted that Fig. 2 shows that the constitutive relationship of the stress ($\sigma_s, s = 1, 2, 3$) and strain ($\varepsilon_s, s = 1, 2, 3$) of a bi-modulus material depends on the local stress state, the modulus should be selected according to the local stress state. For example:

when $0 \geq \sigma_1 \geq \sigma_2 \geq \sigma_3$ (Fig. 2(b)), the material shows isotropic and the compressive modulus should be chosen;

when $\sigma_1 \geq \sigma_2 \geq \sigma_3 > 0$ (Fig. 2(a)), the material shows isotropic and the tensile modulus should be chosen;

when an element is under complicated stress state (Fig. 2(c)), i.e., $\sigma_1 \cdot \sigma_3 < 0$, the material shows transversely isotropic and the unique principal direction of material should be aligned with that of σ_1 if $\sigma_2 < 0$ or σ_3 if $\sigma_2 > 0$. Using material

(a) pure tension   (b) pure compression   (c) complex stress states
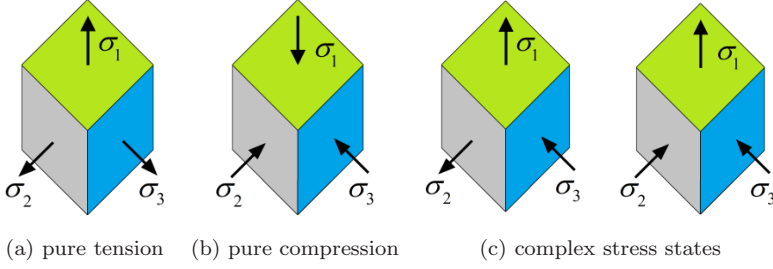
Fig. 2.   Different stress states ($\sigma_1 \geq \sigma_2 \geq \sigma_3$) of a bi-modulus material and the constitutive models: (a) Isotropy with tensile modulus; (b) isotropy with compressive modulus and (c) transversely isotropy.

replacement operation, the elastic modulus depends on the comparison between the values of the tension SED and compression SED, which considers the influence of the second principal stress.

We define tension SED (SED_T) and compression SED (SED_C) as

$$\text{SED}_T = \sum_{u=1}^{t} w_u \cdot \left(\frac{\sum_{G_x=1}^{N_G} w_{G_x} \sum_{G_y=1}^{N_G} w_{G_y} \sum_{G_z=1}^{N_G} w_{G_z}}{\sum_{G_x=1}^{N_G} w_{G_x} \sum_{G_y=1}^{N_G} w_{G_y} \sum_{G_z=1}^{N_G} w_{G_z}} \right), \quad (11)$$

$$\text{SED}_C = \sum_{u=1}^{t} w_u \cdot \left(\frac{\sum_{G_x=1}^{N_G} w_{G_x} \sum_{G_y=1}^{N_G} w_{G_y} \sum_{G_z=1}^{N_G} w_{G_z}}{\sum_{G_x=1}^{N_G} w_{G_x} \sum_{G_y=1}^{N_G} w_{G_y} \sum_{G_z=1}^{N_G} w_{G_z}} \right). \quad (12)$$

where N_G is the number of one-dimensional Gaussian integral points. w_{G_x} is the weighting coefficient of Gaussian integration. In this study, N_G and $w_{G_x} = w_{G_y} = w_{G_z} = 1$.

The modulus of the rth bi-modulus material can be obtained by comparing the tension SED and compression SED, i.e.,

$$E_j^r = \begin{cases} E_T^r, & \text{if } \text{SED}_T > \text{SED}_C, \\ E_C^r, & \text{if } \text{SED}_T < \text{SED}_C, \\ \max(E_T^r, E_C^r), & \text{others.} \end{cases} \quad (13)$$

2.5. *Modification of local stiffness*

It is noted that material replacement operation provides no influence on local stiffness only when the local stress state is in pure tension or in pure compression. If the local stress state is in complex status, the local stiffness changes and the deformation of the local new isotropic material will be different from that of the original bi-modulus material. Therefore, the local stiffness should be modified so as to obtain

an accurate displacement field for further optimization. Before modification of the local stiffness of the jth finite element, two types of SED are calculated.

The "**new**" SED, which is the SED of the finite element with new isotropic materials under the current stress state at the kth step (of iteration), is defined as

$$\text{SED}_{j,k} = \sum_{u=1}^{t} w_u \left(\frac{\sum_{G_x=1}^{N_G} w_{G_x} \sum_{G_y=1}^{N_G} w_{G_y} \sum_{G_z=1}^{N_G} w_{G_z} \sum_{s=1}^{3} \left(\frac{1}{2}\sigma_s \cdot \varepsilon_s\right)_{G_x G_y G_z}}{\sum_{G_x=1}^{N_G} w_{G_x} \sum_{G_y=1}^{N_G} w_{G_y} \sum_{G_z=1}^{N_G} w_{G_z}} \right). \tag{14}$$

The "**old**" SED, which is SED (effective SED) of the finite element with the old material (i.e., bi-modulus materials) under the same stress state, is defined as

$$\text{SED}_{j,k}^{\text{effective}} = \sum_{r=1}^{m-1} \left\{ \psi_r \cdot \sum_{u=1}^{t} w_u \cdot \frac{\sum_{G_x=1}^{N_G} w_{G_x} \sum_{G_y=1}^{N_G} w_{G_y} \sum_{G_z=1}^{N_G} w_{G_z}}{\sum_{G_x=1}^{N_G} w_{G_x} \sum_{G_y=1}^{N_G} w_{G_y} \sum_{G_z=1}^{N_G} w_{G_z}} \right\}_{j,k} . \tag{15}$$

The value of $\text{sign}_r(\cdot)$ can be calculated by both the current modulus of the rth material and the stress state by using either Eqs. (16) or (17).

(1) If the finite element has compressive moduli at the $(k-1)$th iteration and tensile moduli should be used at the current kth iteration, the value of $\text{sign}_r(\cdot)$ is

$$\text{sign}_r(\sigma_s) = \begin{cases} 1 & \text{if } \sigma_s \geq 0, \\ R_{\text{TCE}}^{(r)} & \text{if } \sigma_s < 0, \end{cases} \tag{16}$$

where $R_{\text{TCE}}^{(r)}$ is the moduli ratio of the rth bi-modulus material.

(2) If the finite element has tensile moduli at the $(k-1)$th iteration and compressive moduli should be used at the current kth iteration, the value of $\text{sign}_r(\cdot)$ is

$$\text{sign}_r(\sigma_s) = \begin{cases} 1 & \text{if } \sigma_s \geq 0, \\ R_{\text{TCE}}^{(r)} & \text{if } \sigma_s < 0. \end{cases} \tag{17}$$

The two SED, i.e., $\text{SED}_{j,k}$ and $\text{SED}_{j,k}^{\text{effective}}$, are equal when the element is under a pure tension or pure compression state. If the finite element is under complicated stress state, the two SEDs are always different. We define

$$M_f = \max \left(10^{-6}, \frac{\text{SED}_{j,k}^{\text{effective}}}{\max(\text{SED}_{j,k}, 10^{-10})} \right), \tag{18}$$

as the modification factor for the local effective stiffness of the jth element at the kth iteration.

The stiffness matrix of the jth element with "new" isotropic materials can be given as [Qin, 2000]

$$\mathbf{k}_j = \int_{v_j} \mathbf{B}_j^T \mathbf{D}_j \mathbf{B}_j dv, \tag{19}$$

where $\boldsymbol{B}_j$ is the strain–displacement operator of element. $\boldsymbol{D}_j$ is the constitutive matrix.

The modified stiffness matrix is expressed as

$$\bar{\mathbf{k}}_j = M_f \mathbf{k}_j = \int_{v_j} \mathbf{B}_j^T (M_f \cdot \mathbf{D}_j) \mathbf{B}_j dv. \tag{20}$$

The modification of the local stiffness can also be understood as a constant to give the secondary adjustment on the design variables in the jth finite element, and will be used for calculating the objective function.

For the lcth loading condition, the objective function should be modified as

$$\overline{c_{\text{lc}}} = \sum_{j=1}^{N_{EL}} u_j^T ((M_f)_{\text{lc}} \mathbf{k}_j) u_j = \sum_{j=1}^{N_{EL}} (M_f)_{\text{lc}} \cdot u_j^T \mathbf{k}_j u_j. \tag{21}$$

2.6. *Sensitivity analysis*

The gradient-based method is used to solve the optimization problem defined in Eq. (4). For simplicity, the sensitivity analysis of the model with only three phase bi-modulus materials is carried out.

For $m = 3$ (two solids plus void), the stiffness matrix of the j-th element is

$$\mathbf{k}_j = [\rho_{2,j}^p (\rho_{1,j}^p E_{1,j} + (1 - \rho_{1,j}^p) E_{2,j}) + (1 - \rho_{2,j}^p) E_{3,j}] k_0 \overset{\text{let}}{=} A_0 k_0. \tag{22}$$

Hence, the first order sensitivity of the stiffness matrix of the jth element is expressed as

$$\frac{\partial \mathbf{k}_j}{\partial \rho_{1,j}} = (p\rho_{1,j}^{p-1} \cdot \rho_{2,j}^p \cdot E_{1,j} - p\rho_{1,j}^{p-1} \cdot \rho_{2,j}^p \cdot E_{2,j}) k_0 \overset{\text{let}}{=} A_1 k_0 = \frac{A_1}{A_0} \mathbf{k}_j, \tag{23}$$

$$\frac{\partial \mathbf{k}_j}{\partial \rho_{2,j}} = \{p\rho_{2,j}^{p-1}[\rho_{1,j}^p E_{1,j} + (1 - \rho_{1,j}^p) E_{2,j}] + (-p\rho_{2,j}^{p-1}) E_{3,j}\} k_0 \overset{\text{let}}{=} \frac{A_2}{A_0} \mathbf{k}_j. \tag{24}$$

Correspondingly, the first-order sensitivity of the structural mean compliance with respect to $\rho_{i,j}$ under the lcth loading condition as

$$\left(\frac{\partial \overline{c_{\text{lc}}}}{\partial \rho_1} \quad \frac{\partial \overline{c_{\text{lc}}}}{\partial \rho_2} \right)_j = \left(\left(\frac{\partial M_f}{\partial \rho_1} \quad \frac{\partial M_f}{\partial \rho_2} \right) - M_f \left(\frac{A_1}{A_0} \quad \frac{A_2}{A_0} \right) \right)_j \cdot u_j^T \mathbf{k}_j u_j, \tag{25}$$

$$\frac{\partial c_w}{\partial \rho_m} = \frac{\partial}{\partial \rho_m} \left[\sum_{\text{lc}=1}^{N_{\text{LC}}} (w_{\text{lc}} \cdot \overline{c_{\text{lc}}})^Q \right]^{1/Q}$$

$$= \left[\sum_{\text{lc}=1}^{N_{\text{LC}}} (w_{\text{lc}} \cdot \overline{c_{\text{lc}}})^Q \right]^{1/Q-1} \left[\sum_{\text{lc}=1}^{N_{\text{LC}}} (w_{\text{lc}} \cdot \overline{c_{\text{lc}}})^{Q-1} \cdot w_{\text{lc}} \frac{\partial \overline{c_{\text{lc}}}}{\partial \rho_m} \right], \tag{26}$$

where

$$\frac{\partial \overline{c_{\text{lc}}}}{\partial \rho_m} = -\left(\frac{M_f \cdot A_m}{A_0} u^T \cdot k \cdot u\right)_{\text{lc}}, \quad (\text{lc} = 1, 2, \ldots, N_{\text{LC}}; m = 1, 2). \quad (27)$$

The volume constraint functions is defined as

$$\begin{cases} V_1(\rho_{1,j}, \rho_{2,j}) = \sum_{j=1}^{n} \rho_{1,j} \cdot \rho_{2,j} \cdot v_j - \bar{V}_1, \\ \\ V_2(\rho_{2,j}) = \sum_{j=1}^{n} \rho_{2,j} \cdot v_j - (\bar{V}_1 + \bar{V}_2). \end{cases} \quad (28)$$

And the sensitivities of volume constraints are

$$\begin{pmatrix} \dfrac{\partial V_1}{\partial \rho_1} & \dfrac{\partial V_1}{\partial \rho_2} \\ \dfrac{\partial V_2}{\partial \rho_1} & \dfrac{\partial V_2}{\partial \rho_2} \end{pmatrix}_j = \begin{pmatrix} \rho_{2,j} v_j & \rho_{1,j} v_j \\ 0 & v_j \end{pmatrix}. \quad (29)$$

2.7. *Optimization procedure*

The Method of Moving Asymptotes (MMA) [Svanberg, 1987] is adopted to solve the present optimization problem. The PDEs are solved using the finite element method. In each simulation circle, the initial elastic moduli of elements are the same tension modulus of the first solid material (M1). All the initial design variables are considered to be equal. The process of optimization is as follows.

(1) Create finite element model for a structure to be optimized. Let $k = 1$, and initialize the design domain;
(2) Perform the finite element analysis of structure under MLC;
(3) Calculate the SED, SED_T, SED_C and the local effective SED (Eqs. (11), (12), (14) and (15)) of each element;
(4) Update the elastic moduli of materials in each element (Eq. (13));
(5) Obtain M_f for each element according to Eq. (18);
(6) Calculate the objective and constraint functions and their first-order sensitivities (Eqs. (21), (25), (28) and (29));
(7) Update the design variables using MMA;
(8) Check the convergence: if Eq. (30) is not satisfied, $k = k+1$ return to step (2), else go to next step;
(9) Save and stop.

The termination criterion is either defined by maximum iteration number $k_{\max} < 150$ or the change of compliance of the structure satisfied

$$\left|\frac{C_t}{C_k} - 1\right| \leq \eta, \quad t = k - 1, \ k - 2, \ldots, k - kn. \quad (30)$$

The iteration stops when the convergence criterion is satisfied. η is the algorithm tolerance, which is 0.001 in the present simulations, and $kn = 5$.

3. Examples and Discussion

In the following examples, the computer code is compiled with MATLAB and integrated with the commercial software ANSYS 12.0 [Ansys, 2013] for structural optimization analysis. The objective is to minimize the compliance of the structure within the design domain. In each example, there are two bi-modulus solids (M1 in red and M2 in yellow) and void (M3 in white) in the optimization. The Poisson's ratio is 0.2 for both solids. The tensile moduli of the two solids are 80 and 40 GPa, respectively. Except in *Example* 4, the values of R_{TCE} of M1 and M2 are 2 and 0.5, respectively. It means that the two solids have the same highest magnitude of modulus and the same lowest magnitude of modulus.

3.1. *Example* 1

In Fig. 3, a deep wall with 3-m high and 9-m span is discretized into 30×90 square plane stress elements. The wall is under three loading cases. In the major load case, there is a concentrated force, P_1, is applied at the central point K_1 on the top side of the wall. In the second load case, a compressive concentrated force $P_2 = 0.01P_1$ is applied at point K_2 and is normal to the top side. In the third load case, the tensile force $P_3 = P_2$ is applied at point K_3 and is normal to the top side, too. All the loading cases have the same weighting coefficient. The volume ratios of the two solids (M1 and M2) and void (M3) are 0.15, 0.15 and 0.70, respectively.

Figure 4 shows the final distributions of materials with different values of Q. In each case, the layouts of solid materials are asymmetry, which is due to two factors. One is the asymmetry of the three loads on the symmetric structure. The other is that the volume ratios of the two solids are identical and, simultaneously, the tension modulus of M1 is equal to the compression modulus of M2. Therefore, the major part of M1 is layout to support the tensile loads, and most of M2 is on the path for supporting compressive loads.
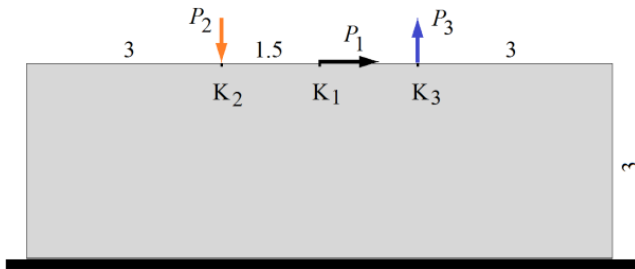

Fig. 3.   Initial design of a wall.

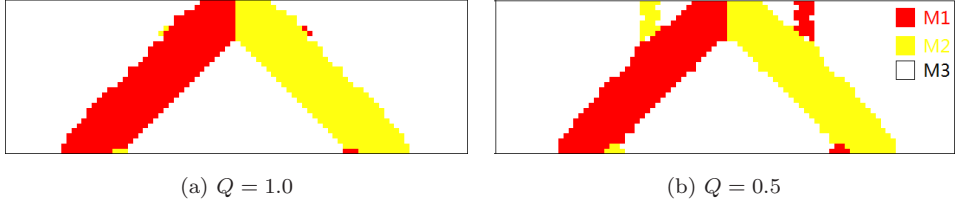(a) $Q = 1.0$ (b) $Q = 0.5$

Fig. 4.   Diagram of multi-phases materials in a finite element.

However, in the first case ($Q = 1$), there is no material in the final structure to support two weak loads, i.e., P_2 and P_3. If, for example, the two loads are important in operation of the structure, the final materials layout in Fig. 4(a) is invalid. This is actually the drawback of traditional (linear) weighting approach for solving ill-loaded topology optimization.

As we set $Q = 0.5$, i.e., a fractional norm weighting scheme being adopted, the final materials layout (Fig. 4(b)) looks reasonable. For example, the two weak loads are supported by M1 and M2, respectively. P_2 is compressive load, and is supported by M2 which has higher compressive modulus than that of M1. Similarly, P_3 is supported by M3. Because the total amount of the two solids are the same in the two final structures, the two oblique arms in Fig. 4(b) are thinner than those in Fig. 4(a).

3.2. *Example 2*

The structure shown in Fig. 5 is a cantilever beam whose dimension is $0.7\,\mathrm{m}$ (span) $\times 0.4\,\mathrm{m}$ (height)$\times 0.02\,\mathrm{m}$ (thickness). In numerical analysis, the structure is modeled with 98×56 elements. The whole design domain is divided into four rectangle subdomains, i.e., I, II, III and IV, with the same side length. There are two loading cases applied on the structure. In the first case, the concentrated force P_1 is applied at the center (K_1) of structure. In the second case, the concentrated force P_2 is applied at the center (K_2) of free end. The volume fractions of M1, M2 and M3 are 0.18, 0.18 and 0.64, respectively. Both cases have the same weighting coefficient.

Two schemes are considered. (a) $P_1 = 0.01P_2 = 20\mathrm{N}$; (b) $P_1 = 100P_2 = 2000\mathrm{N}$.

In Fig. 6(a), the final structure is obtained when only the load P_2 is considered. Obviously, the structure can also be used to support the load P_1 at the center of structure. Hence, the final structure is always valid whether $P_2 \gg P_1$ or not. At the same time, the two materials are layout according to the criterion: M1 (red) is mainly under tension status and M2 (yellow) is under compression status because of their bi-modulus behavior.

In Fig. 6(b), the final structure is obtained when we only consider the load P_1. We find that the two solids appear in subdomains I and II only. Hence, the structure cannot be used to support P_2.
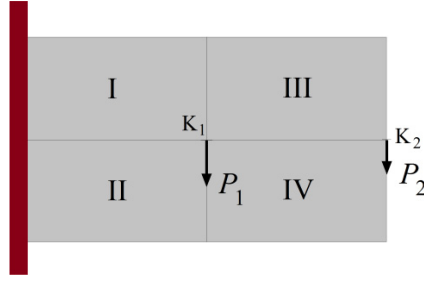
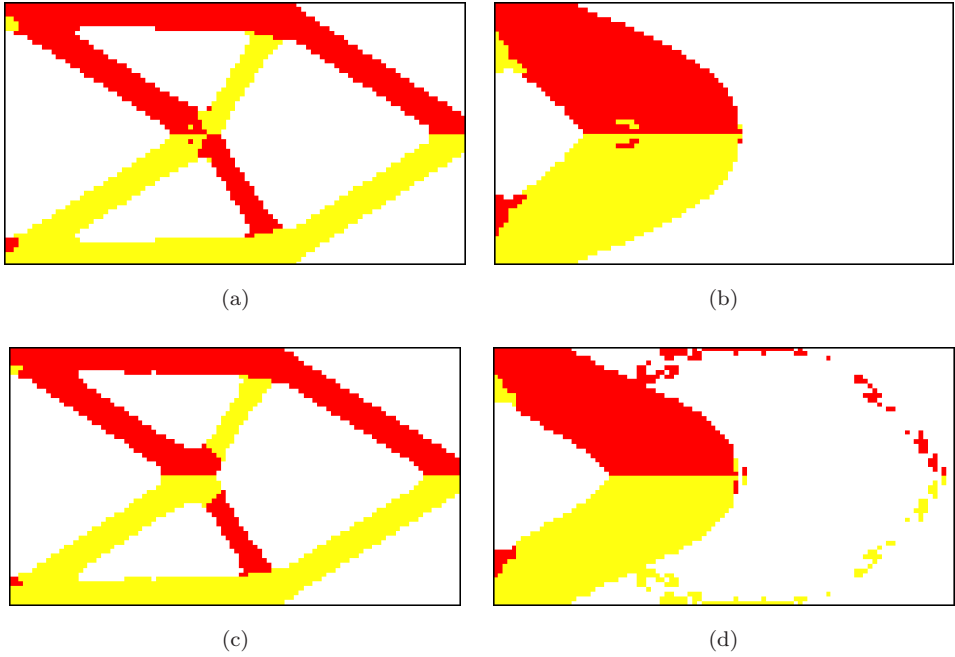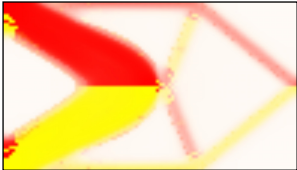Fig. 5.   Initial design of a cantilever beam under MLC.

Fig. 6.   Optimal materials layouts in the final structure under different loading conditions: (a) Only under $P_2 = 2000$N; (b) only under $P_1 = 2000$N; (c) under MLC with $P_2 = 2000$N ($Q = 1$); (d) under MLC with $P_1 = 2000$N ($Q = 1$).

If the structure is under MLC and $P_1 \ll P_2$, the final structure is shown in Fig. 6(c), which is slightly different from Fig. 6(a). The structure can support both strong and weak loads simultaneously. In this condition, we do not call the structure is under ill loads. If $P_2 \ll P_1$, the final structure is shown in Fig. 6(d) at $Q = 1$. Obviously, the amount of materials on the path to support P_2 is too low. The structure shown in Fig. 6(d) can be considered under ill loads. If we need a reasonable solution, the value of Q should be less than 1.0.

Table 1.   Optimal layouts of multiple bi-modulus materials in the final structure with respect to different values of Q (An element with relative density less than threshold is shown in white).

Q	Threshold is 0	Threshold is 1.0
1.0		
0.5		
0.25		

To achieve a suitable layouts of materials in the structure under ill-loaded cases, i.e., $P_1 = 2000$N and $P_2 = 20$N, we adopt different values of Q in simulation, and the final materials layout are shown in Table 1. Hence, the final structure with respect to $Q = 0.5$ can be used when we accept the structure with mid-density elements. Commonly, we do not use such structure as the final design due to complicated manufacturing. If we set $Q = 0.25$, the final structure with only solid elements can be accepted as the final design. From Fig. 7, we find that the values of objective function are 0.0321 ($Q = 1.0$), 0.0339 ($Q = 0.5$) and 0.0391 N.m ($Q = 0.25$), respectively. The value of objective function at $Q = 0.25$ is about 22% higher than that at $Q = 1.0$. This is mainly because the amount of material to support P_1 at $Q = 0.25$ is lower than that at $Q = 1.0$.

3.3. *Example 3*

Consider a simply-supported beam shown in Fig. 8 whose dimension is 1.0 (span) $\times$ 0.5. The structure is discretized with 100×50 finite elements. The structure is subjected to two loading cases. In the first loading case, the two concentrated forces, P_1 and P_2, are applied vertically on the upper side symmetrically, e.g., P_1 at point K_1 (1/10 of span) and P_2 at point K_2 (9/10 of span), respectively. $P_1 = P_2 = 2$N. In the second loading case, a concentrated force, $P_3 = 1000P_2$, is applied at the center of the lower side of the beam. The volume ratios of the two solids and void
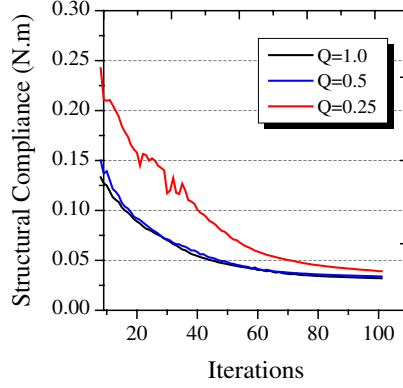
Fig. 7.   Iteration histories of structural compliance with respect to different values of Q.
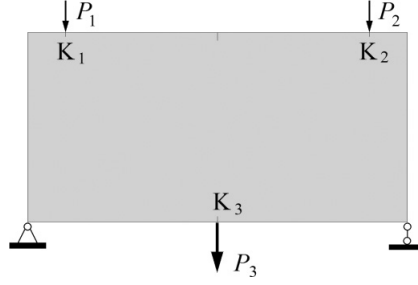

Fig. 8.   Design domain of deep beam.

are 0.1, 0.2 and 0.7, respectively. Both weighting coefficients for loading cases are identical. The effect of the value of Q on the final multi-materials distribution is investigated.

Figure 9 shows the final materials distribution in the design domain with respect to different values of Q. As the two forces, P_1 and P_2, in the first loading case is far less than P_3 in the second case, there is no material to support P_1 and P_2 (Fig. 9(a)) when the linear weighting scheme is adopted ($Q = 1$). One can also find that the solution shown in Fig. 9(b) (with respect to $Q = 0.5$) are the same as that in Fig. 9(a). That is because the weak forces still have very small influence on the materials distribution due to the value of Q being not small enough. When $Q = 0.2$, the influence of weak forces on the final distribution increases significantly and the amount of materials to support them becomes larger. Hence we consider the solution in Fig. 9(c) to be valid for manufacturing. If we choose much smaller value of Q, e.g., $Q = 0.1$, the weak forces (P_1 and P_2) have greater influence on the final materials distribution than the stronger force (P_3). And the topology of the structure is different from traditional design (Fig. 9(a)), obviously.

(a) $Q = 1.0$

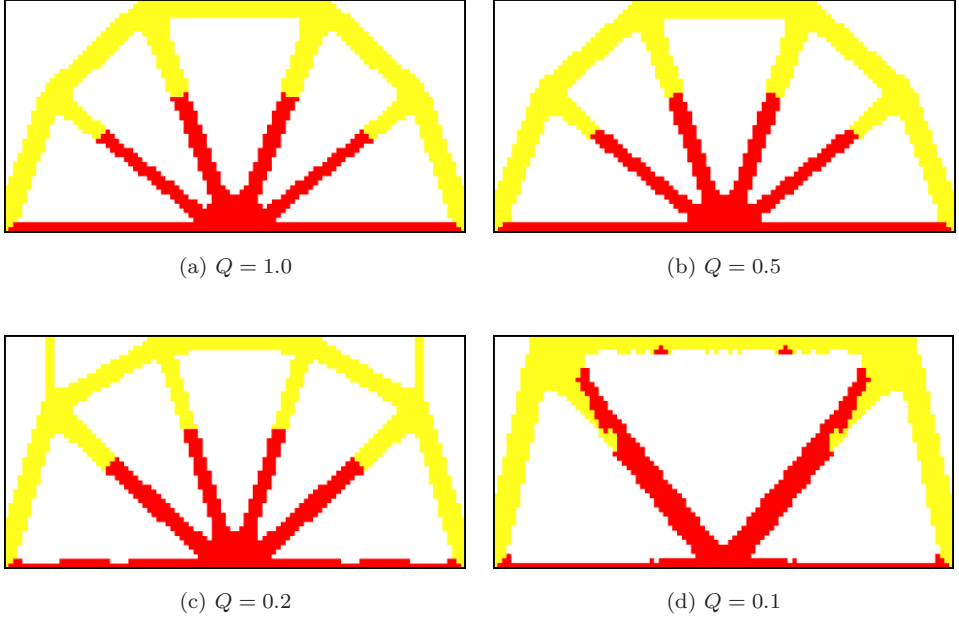(b) $Q = 0.5$

(c) $Q = 0.2$

(d) $Q = 0.1$

Fig. 9.   Optimal materials layout in the beam structure with respect to different values of Q.

As the tensile modulus of M1 (red) is greater than that of M2 (yellow), M1 is mainly distributed near the bottom of the structure. Because the amount of M2 is greater than M1, most of M2 is under compression, at which state M2 behaves isotropic with $E_C > E_T$. One can also find that the amount of M1 in the inner oblique bars is much greater than that of M2 as the Q is very small, e.g., $Q = 0.1$.

3.4. *Example 4*

The L-shape structure shown in Fig. 10(a) has three square subdomains (I, II and III) with sizes of $1\,\mathrm{m(span)} \times 1\,\mathrm{m(height)} \times 0.02\,\mathrm{m}$ (thickness). Each square subdomain is meshed with 32×32 elements. The top side of the structure is fixed. There are two loading cases applied on the structure. In the first case, the concentrated force P_1 is applied at the point K_1. In the second case, the concentrated force P_2 is applied at the point K_2. $P_1 = 100\,P_2 = 20000\mathrm{N}$. There are three phases (M1, M2 and M3) with the volume fractions of 0.08, 0.22 and 0.7, respectively. The tensile moduli of the M1 and M2 are 80 and $40\,\mathrm{GPa}$, respectively. M3 is void. The values of R_{TCE} of M1 and M2 are 5 and 0.2, respectively.

As the value of P_2 is only 1% of that of P_1, there is no material to support the weaker load, i.e., P_2, when using traditional SIMP method ($Q = 1.0$). Hence, the present problem is a typical ill-loaded topology optimization problem. When adopting the present scheme, i.e., fraction-norm scheme, to deal with the problem, one can find that there will appear material on the path to support the weaker load. For example, when $Q = 0.5$, the final materials layout are shown in Fig. 10(c),

(a) Initial design of L-shape structure

(b) $Q = 1$
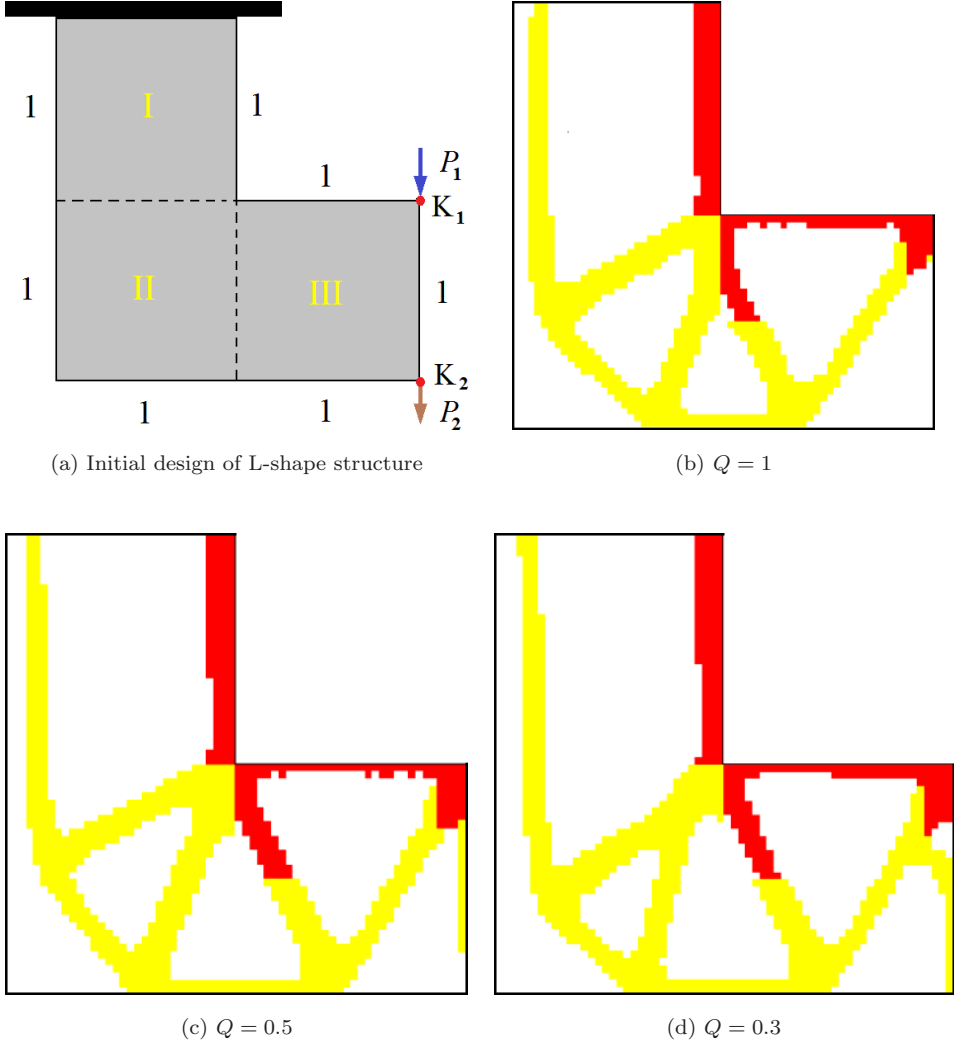

(c) $Q = 0.5$

(d) $Q = 0.3$

Fig. 10. Materials layout in the L-shape structure: (a) Initial design of the structure; (b)–(d) the optimal materials layout in the design domain when $Q = 1.0, 0.5$ and 0.3, respectively.

in which there is a yellow bar existing on the right side of subdomain III. Due to the lower volume ratio of M2 (yellow) and higher value of Q, the bar seems shorter than 1. As we reduce the value of Q, for example, to be 0.3, the path to support the weaker load is very clear. This can be verified when one compares the right side of subdomain III in Figs. 10(c) and 10(d). Due to more materials are on the path to support P_2, the materials layout in the other two subdomains are also different. For example, the distances of M2-bar in the subdomain I to the left boundary are not identical for the three figures with respect to different values of Q.

4. Conclusion

Major headings should be typeset in boldface with the first letter of important words capitalized.

For a structure under MLC with ill loads, the scheme of linear weighted generalized objective function is infeasible in solving topology optimization of the structure with multiple bi-modulus materials. The reason is that the weak loads (i.e., ill loads) are far less than the stronger loads and, simultaneously, not on the LTP of the stronger loads. There is no material to support the weak loads in the final structure obtained using linear weighting scheme. To enhance the influence of weak loads on the objective function, in this paper, a Q-norm weighting scheme is adopted. Meanwhile, the material replacement approach is used to simplify topology optimization of bi-modulus materials. Numerical examples demonstrated the feasibility of the present method and some conclusions can be drawn.

(1) The final solid frame in the design domain mainly depends on the loading cases and the value of Q. But the final layouts of the bi-modulus materials depends on the moduli differences among the materials, e.g., the materials with higher tensile moduli appear on the LTPs under tension state and the materials with higher compressive moduli are on the path to support compression loads;

(2) The lower value of Q, the higher contribution of the weak loads on the generalized objective function, and, the more material to support the weak loads;

(3) Generally, the value of Q in [0.2, 0.5] are suggested in most ill-loaded cases for finding a feasible solution.

Acknowledgment

References

Achtziger, W. [1996] "Truss topology optimization including bar properties different for tension and compression," *Structural Optimization* **12**(1), 63–74.

Allaire, G., Dapogny, C., Delgado, G. and Michailidis, G. [2013] "Multi-phase structural optimization via a level set method," *ESAIM: Control, Optimisation and Calculus of Variations* **20**, 576–611.

Ambartsumyan, S. [1965] "The axisymmetric problem of circular cylindrical shell made of materials with different stiffness in tension and compression," *Izvestiya Akademiya Nauk SSSR, Mekhanika* **4**, 77–85.

Ansys [2013] http://www.ansys.com, 2013 (assessed April 2015),

Bathe, K.-J. [2006] *Finite Element Procedures* (Klaus-Jurgen Bathe, United States of America).

Blasques, J. P. and Stolpe, M. [2012] "Multi-material topology optimization of laminated composite beam cross sections," *Composite Structures* **94**(11), 3278–3289.

Bruggi, M. [2014] "Finite element analysis of no–tension structures as a topology optimization problem," *Structural and Multidisciplinary Optimization* **50**(6), 957–973.

Bruggi, M. and Duysinx, P. [2013] "A stress-based approach to the optimal design of structures with unilateral behavior of material or supports," *Structural and Multidisciplinary Optimization* **48**(2), 311–326.

Cai, K. [2011] "A simple approach to find optimal topology of a continuum with tension-only or compression-only material," *Structural and Multidisciplinary Optimization* **43**(6), 827–835.

Cai, K., Gao, Z. L. and Shi, J. [2013] "Topology optimization of continuum structures with bi-modulus materials," *Engineering Optimization* **46**(2), 244–260.

Cai, K. and Shi, J. [2008] "A heuristic approach to solve stiffness design of continuum structures with tension/compression-only materials," *Fourth International Conference on Natural Computation*, **1**, Jinan, China, pp. 131–135.

Cai, K., Shi, J. and Zhang, A. [2014] "Stiffness design of a continuum under ill-load cases by fractional-norm objective formulation," *Optimization and Engineering* **15**(4), 927–944.

Chang, C. J., Zheng, B. and Gea, H. C. [2007] "Topology optimization for tension/compression only design," *Proceedings of the 7th World Congress on Structural and Multidisciplinary Optimization*, Vol. 4, Seoul, South Korea, pp. 2488–2495.

Diaz, A. R. and Bendsøe, M. P. [1992] "Shape optimization of structures for multiple loading conditions using a homogenization method," *Structural Optimization* **4**(1), 17–22.

Dorn, W. S. [1964] "Automatic design of optimal structures," *Journal de Mecanique* **3**, 25–52.

Du, Z. L. and Guo, X. [2014] "Variational principles and the related bounding theorems for bi-modulus materials," *Journal of the Mechanics and Physics of Solids* **73**, 183–211.

Dühring, M. B., Jensen, J. S. and Sigmund, O. [2008] "Acoustic design by topology optimization," *Journal of Sound and Vibration* **317**(3–5), 557–575.

Forsberg, J. and Nilsson, L. [2007] "Topology optimization in crashworthiness design," *Structural and Multidisciplinary Optimization* **33**(1), 1–12.

Gersborg-Hansen, A., Sigmund, O. and Haber, R. B. [2005] "Topology optimization of channel flow problems," *Structural and Multidisciplinary Optimization* **30**(3), 181–192.

Gibiansky, L. V. and Sigmund, O. [2000] "Multiphase composites with extremal bulk modulus," *Journal of the Mechanics and Physics of Solids* **48**(3), 461–498.

Guo, X., Zhang, W. and Zhong, W. [2014a] "Doing topology optimization explicitly and geometrically — A new moving morphable components based framework," *Journal of Applied Mechanics* **81**(8), 081009.

Guo, X., Zhang, W. and Zhong, W. [2014b] "Explicit feature control in structural topology optimization via level set method," *Computer Methods in Applied Mechanics & Engineering* **272**(2), 354–378.

Han, S. Y. and Lee, S. K. [2005] "Development of a material mixing method based on evolutionary structural optimization," *JSME International Journal Series A* **48**(3), 132–135.

Hvejsel, C. F. and Lund, E. [2011] "Material interpolation schemes for unified topology and multi-material optimization," *Structural and Multidisciplinary Optimization* **43**(6), 811–825.

Jang, G.–W., Kim, K. J. and Kim, Y. Y. [2008] "Integrated topology and shape optimization software for compliant MEMS mechanism design," *Advances in Engineering Software* **39**(1), 1–14.

Jones, R. M. [1977] "Stress-strain relations for materials with different moduli in tension and compression," *AIAA Journal* **15**(1), 16–23.

Kanno, Y. [2011] *Nonsmooth Mechanics and Convex Optimization* (CRC Press, Taylor & Francis Group, Boca Raton, FL).

Liu, S. T. and Qiao, H. T. [2010] "Topology optimization of continuum structures with different tensile and compressive properties in bridge layout design," *Structural and Multidisciplinary Optimization* **43**(3), 369–380.

Luo, Y. J. and Kang, Z. [2013] "Layout design of reinforced concrete structures using two-material topology optimization with Drucker–Prager yield constraints," *Structural and Multidisciplinary Optimization* **47**(1), 95–110.

Luo, Y. J., Wang, M. Y. and Kang, Z. [2015] "Topology optimization of geometrically non-linear structures based on an additive hyperelasticity technique," *Computer Methods in Applied Mechanics & Engineering* **286**, 422–441.

Luo, Z., Yang, J. Z., Chen, L. P., Zhang, Y. Q. and Abdel-Malek, K. [2006] "A new hybrid fuzzy-goal programming scheme for multi-objective topological optimization of static and dynamic structures under multiple loading conditions," *Structural and Multidisciplinary Optimization* **31**(1), 26–39.

Mei, Y. L. and Wang, X. M. [2004] "A level set method for structural topology optimization with multi-constraints and multi-materials," *Acta Mechanica Sinica* **20**(5), 507–518.

Natasha, V., Georgios, M., Guillaume, P., Rafael, E., Grégoire, A. and Bréchet, Y. [2014] "Material interface effects on the topology optimizationof multi-phase structures using a level set method," *Structural and Multidisciplinary Optimization* **50**(4), 623–644.

Qin, Q. H. [1994] "Hybrid Trefftz finite-element approach for plate bending on an elastic foundation," *Applied Mathematical Modelling* **18**(6), 334–339.

Qin, Q. H. [1995] "Hybrid-Trefftz finite element method for Reissner plates on an elastic foundation," *Computer Methods in Applied Mechanics and Engineering* **122**(3–4), 379–392.

Qin, Q. H. [2000] *The Trefftz Finite and Boundary Element Method* (WIT Press, Southampton).

Qin, Q. H. [2005] "Trefftz finite element method and its applications," *Applied Mechanics Reviews* **58**(5), 316–337.

Qin, Q. H. and He, X. Q. [1995] "Variational principles, FE and MPT for analysis of non-linear impact-contact problems," *Computer Methods in Applied Mechanics and Engineering* **122**(3), 205–222

Querin, O. M., Victoria, M. and Martí, P. [2010] "Topology optimization of truss-like continua with different material properties in tension and compression,"*Structural and Multidisciplinary Optimization* **42**(1), 25–32.

Ramani, A. [2009] "A pseudo-sensitivity based discrete-variable approach to structural topology optimization with multiple materials," *Structural and Multidisciplinary Optimization* **41**(6), 913–934.

Seldin, E. [1966] "Stress–strain properties of polycrystalline graphites in tension and compression at room temperature," *Carbon* **4**(2), 177–191.

Sigmund, O. and Torquato, S. [1999] "Design of smart composite materials using topology optimization," *Smart Materials and Structures* **8**(3), 365–379.

Stegmann, J. and Lund, E. [2005] "Discrete material optimization of general composite shell structures," *International Journal for Numerical Methods in Engineering* **62**(14), 2009–2027.

Sui, Y., Yang, D. and Wang, B. [2000] "Topological optimization of continuum structure with stress and displacement constraints under multiple loading cases," *Acta Mechanica Sinica* (2), 171–179.

Svanberg, K. [1987] "The method of moving asymptotes — A new method for structural optimization," *International Journal for Numerical Methods in Engineering* **24**(2), 359–373.

Wang, M. Y. and Wang, X. M. [2004] "Color' level sets: A multi-phase method for structural topology optimization with multiple materials," *Computer Methods in Applied Mechanics and Engineering* **193**(6–8), 469–496.

Wang, M. Y. and Zhou, S. W. [2005] "Synthesis of shape and topology of multi-material structures with a phase-field method," *Journal of Computer-Aided Materials Design* **11**(2–3), 117–138.

Yang, Y., Moen, C. D. and Guest, J. K. [2014] "Three-dimensional force flow paths and reinforcement design in concrete via stress-dependent truss-continuum topology optimization," *Journal of Engineering Mechanics* **141**(1) 10.1061/(ASCE)EM.1943-7889.0000819.

Zenkert, D. and Burman, M. [2009] "Tension, compression and shear fatigue of a closed cell polymer foam," *Composites Science and Technology* **69**(6), 785–792.

Zhou, M. and Wang, M. Y. [2013] "Engineering feature design for level set based structural optimization," *Computer-Aided Design* **45**(12), 1524–1537.

Zhou, S. and Wang, M. Y. [2006] "Multimaterial structural topology optimization with a generalized Cahn–Hilliard model of multiphase transition," *Structural and Multidisciplinary Optimization*: **33**(2), 89–111.

Zhuang, C. G., Xiong, Z. H. and Ding, H. [2007] "A level set method for topology optimization of heat conduction problem under multiple load cases," *Computer Methods in Applied Mechanics and Engineering* **196**(4–6), 1074–1084.